

Synthesis and characterization of novel 4-phenylpyridine unit based alkaline anion exchange membranes†

Di Lu,^{ab} Lele Wen^{*ac} and Lixin Xue^{*a}

For exploring more types of suitable polymeric membranes for application in alkaline fuel cells (AFCs), a series of 1,2-dimethylimidazolium functionalized poly(arylene ether sulfone)s containing 4-phenylpyridine units in the main chain (named as DIm-PPYPAES) were firstly synthesized as anion exchange membranes (AEMs) in this work. Proton nuclear magnetic resonance (¹H NMR) and Fourier transform infrared (FT-IR) spectroscopy were employed to characterize and confirm the chemical structure of the synthesized copolymers and the derived membranes. The DIm-PPYPAES membranes with different ionized levels ranging from 1.15 meq. g⁻¹ to 1.77 meq. g⁻¹, exhibited good thermal stability, solubility behavior and a relatively high level of hydroxide conductivity. The highest hydroxide conductivity of 83.35 mS cm⁻¹ at 80 °C was achieved for the DIm-PPYPAES-4 membrane with a moderate IEC of 1.77 meq. g⁻¹. Moreover, after 15 days of treatment with a 2 M NaOH solution at 60 °C, the DIm-PPYPAES membrane still exhibited relatively high ionic conductivity even above 10 mS cm⁻¹ at 30 °C and retained their integrated shapes.

1. Introduction

Polymer electrolyte fuel cells (PEFCs) have attracted considerable attention due to their high energy efficiency, relatively low operation temperature and low cost.^{1,2} As is well known, the polymer electrolyte membrane is critical for the performance of the whole cell system, which not only separates the fuel, but also transports ions to complete the electrical circuit. At present, as one type of polymer electrolyte membrane, the proton electrolyte membranes (PEMs) based on perfluorinated ionomers, such as Nafion®, are representative membranes and have been greatly developed. However, the large-scale application of proton electrolyte membrane fuel cells (PEMFCs) is still hindered by the high production cost of membranes and precious metal catalysts (Pt).³ As one class of alternative

polymer electrolyte fuel cells, anion exchange membrane fuel cells (AEMFCs) exhibit potential advantages, including faster oxygen reduction reaction kinetics and employment of non-precious metal catalysts (Ni, Co) in AEMFCs. More importantly, perfluorinated polymer-based PEMs could be replaced by a series of non/partially fluorinated polymer-based anion exchange membranes (AEMs) in fuel cells. These merits significantly enhance the cell efficiency and reduce the production cost of the fuel cell.

In general, the benchmark of AEMs for practical application in fuel cells should possess sufficiently high ionic conductivity (>10 mS cm⁻¹), high dimensional stability as well as good durability under harsh operating conditions (high pH and elevated temperature environment).^{4,5} In recent years, the state-of-the-art AEM materials are mainly focused on the development of various types of polymer backbones, such as poly(styrene)s,^{6,7} poly(phenylene oxide)s,⁸⁻¹² poly(phenylene)s,¹³ polybenzimidazoles,¹⁴ poly(arylene ether sulfone)s,¹⁵⁻¹⁹ poly(arylene ether ketone)s,²⁰ and so forth. To increase the ionic conductivity, a common strategy used is *via* increasing the ion exchange capacity (IEC) of the membranes. However, it has been reported that an over-high IEC value usually causes poor dimensional stability, which is disadvantageous to the lifespan of the membranes.²¹ To restrict the swelling of polymeric membranes, the self-crosslinking route is an effective solution at the expense of the solubility of the membranes in organic solvents.^{22,23}

In order to enhance the ionic conductivity of AEMs with a reasonable ionic level, very recently, Zhuang *et al.* and other

^aPolymer and Composite Division, Zhejiang Key Laboratory of Marine Materials and Protective Technologies, Ningbo Institute of Material Technology and Engineering, Chinese Academy of Sciences, Ningbo, Zhejiang, 315201, P. R. China. E-mail: wenlele@nimte.ac.cn; xuelx@nimte.ac.cn

^bDepartment of Chemistry, College of Science, Shanghai University, Shanghai, 200444, P. R. China

^cKey Laboratory of Organofluorine Chemistry, Shanghai Institute of Organic Chemistry, Chinese Academy of Sciences, Shanghai, 200032, P. R. China

researchers adopted the strategy of self-aggregation to achieve high ionic conductivity by introducing long and hydrophobic side chains onto the polymer backbones.^{11,12,21,24} Due to the flexibility of the side chains, long alkyl chains give rise to the loose and random stack of polymer chains, which facilitate the self-aggregation of ionic clusters. In addition to the introduction of alkyl side chains onto the polymers, employing the rigid multi-aromatic monomers pendant with bulky groups is another effective way to increase the free volume of polymeric chains, which might enhance the impact of self-aggregating.²⁵ Although a variety of examples have been reported, most of the aromatic moieties, including fluorene,^{26–30} phenolphthalein (PPH),^{31,32} tetraphenyl methane^{33,34} as well as phthalazinone,^{35,36} were incorporated as hydrophilic segments in the membranes. Besides the aforementioned aromatic scaffolds, it is noteworthy that the pyridine ring pendant with an aromatic analogue is a class of good candidates to constitute polymer backbones, which could also intensify the effect of the self-aggregating and improve the OH[−] conducting efficiency. Meanwhile, it is well known that the incorporation of a pyridine moiety in the polymer backbone is advantageous to the improvement of thermal stability, chemical stability, processability and retention of the mechanical property of the resulting polymer to some extent.^{37,38}

Herein, we report on the synthesis and characterization of a new class of anion exchange membranes based on the poly(arylene ether sulfone)s containing 4-phenyl-pyridine unit in the main chain. Novel 4-phenyl-2,6-bis(4-hydrophenyl)pyridine (PPY) was synthesized as one of the monomers to constitute the hydrophobic segments of the copolymer. Considering that the 1,2-dimethylimidazolium group possesses good chemical stability because of its steric effect, the 1,2-dimethylimidazolium ring is utilized as a pendant ionic group to form the hydrophilic domains of the membranes.³⁹ For comparison of the performance of this class of AEMs, one kind of 1,2-dimethylimidazolium functionalized membrane without the PPY unit (DIm-PSF) as a known comparison was prepared as well. A comprehensive study on the properties of the membranes, including thermal stability, the mechanical property, ion exchange capacity, water uptake and dimensional stability, as well as chemical stability under alkaline conditions were investigated.

2. Experimental

2.1 Materials

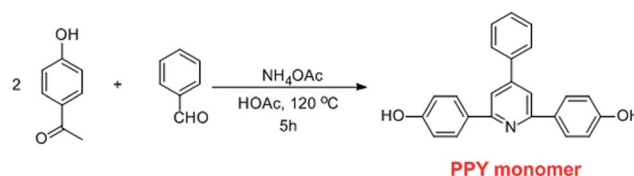
4'-Hydroxyacetophenone (98%, Aladdin, China), 4,4'-biphenol (98%, Aladdin, China), benzaldehyde (>99%, Aladdin, China), ammonium acetate (AR, Aladdin, China), acetate (>99%, Aladdin, China), 2,2-bis(4-hydroxy-3,5-dimethylphenyl)propane (HDPP) (98%, TCI, Japan), bis(4-fluorophenyl) sulfone (FPS) (99%, TCI, Japan), potassium carbonate (99%, Aladdin, China), benzoyl peroxide (BPO) (99%, Aladdin, China), *N*-bromosuccinimide (NBS) (99%, Aladdin, China), 1,2-dimethylimidazole (98%, Aladdin, China) and tetramethylene sulfone (98%, Aladdin, China) were used as received. Toluene (99%, Aladdin, China) and *N,N*-dimethylacetamide (DMAc) (98%, Aladdin,

China) were dried by refluxing over CaH₂. All other chemicals were purchased from Sinopharm Chemical Reagent Co. and used without further purification.

2.2 Preparation of the DIm-PPYPAES membranes

2.2.1 Synthesis of monomer 4-phenyl-2,6-bis(4-hydrophenyl)pyridine (PPY). Monomer PPY was synthesized according to the modified Chichibabin pyridine synthesis method.³⁹ To a 250 mL three necked flask was added 4-hydroxyacetophenone (41.4 g, 0.3 mol), benzaldehyde (15.9 g, 0.15 mol), ammonium acetate (92 g) and glacial acetic acid (200 mL). The mixture was heated at 120 °C with stirring under Ar atmosphere for 5 h. Then the resulting red solution was cooled to room temperature and poured into 500 mL of deionized water, forming a pale yellow viscous solid. Afterwards, the crude product was dissolved in a 10% NaOH aqueous solution, and the insoluble solid was filtered off and excess of glacial acetic acid was added dropwise to this alkaline solution until no more yellow precipitate formed. The pure monomer compound was obtained after recrystallization (ethyl acetate/petroleum ether) and drying at 50 °C under vacuum as a pale yellow powder (yield: 72%). The desired monomer was confirmed by ¹H NMR spectroscopy (Fig. S1†). ¹H NMR (400 MHz, DMSO-d₆): δ 9.74 (s, 2H), 8.15 (d, 4H, *J* = 8.0 Hz), 7.97 (d, 2H, *J* = 8.0 Hz), 7.95 (s, 2H), 7.54 (m, 3H), 6.90 (d, 4H, *J* = 8.0 Hz). The reaction procedure is illustrated in Scheme 1.

2.2.2 Synthesis of poly(arylene ether sulfone)s containing 4-phenyl-pyridine unit (PPYPAES). The typical procedure for the synthesis of the PPYPAES polymer is as follows. The PPY monomer (1.1879 g, 3.5 mmol), HDPP (995.4 mg, 3.5 mmol), FPS (1.7798 g, 7 mmol), potassium carbonate (2.4185 g, 17.5 mmol), tetramethylene sulfone (13 mL) and toluene (15 mL) were placed into a 100 mL three-necked round bottom flask equipped with a Dean-Stark trap, a condenser, a mechanic stirrer and a gas inlet and outlet. The reaction mixture was carried out at 150 °C for 2 h under nitrogen flow to remove the water in the solution. Then the temperature was raised to 210 °C for 3 h to yield a viscous brown mixture. The mixture was poured into 200 mL of aqueous methanol (methanol/deionized water = 1/1) to produce an off-white resin. The as-prepared copolymer PPYPAES, which represents the 4-phenyl-pyridine (PPY) moiety containing the poly(arylene ether sulfone)s (PAES) polymer, was obtained (3.75 g) after washing with deionized water and methanol several times, and then dried *in vacuo* at 70 °C overnight.



Scheme 1 Synthesis of 4-phenyl-2,6-bis(4-hydrophenyl)pyridine (PPY) monomer.

2.2.3 Bromination of PPYPAES. The radical bromination reaction of the benzyl methyl-bearing PPYPAES was carried out in 1,1,2,2-tetrachloroethane (TCE) using NBS and benzoyl peroxide as the bromination agent and initiator, respectively. A typical procedure for the preparation of B-PPYPAES is as follows. Firstly, 1.5 g of PPYPAES and 30 mL of TCE were added to a 100 mL three-necked round bottomed flask and heated to 80 °C under nitrogen atmosphere, followed by addition of NBS (801 mg, 4.5 mmol) and BPO (55 mg, 0.225 mmol) to the reaction solution after the polymer completely dissolved. The reaction mixture was stirred at 80 °C for 6 h, and then, the solution was cooled to room temperature and poured into 200 mL of methanol solution to give a white fibrous precipitate. The brominated product B-PPYPAES (where B refers to the brominated compound) was collected (1.35 g) after filtration and drying *in vacuo* at 70 °C overnight.

2.2.4 Fabrication of the membranes. The typical procedure for the quaternization of B-PPYPAES is as follows. B-PPYPAES (0.5 g) was dissolved in DMAc (5.0 g) to form a 9 wt% solution; after the polymer was dissolved completely, 1,2-dimethylimidazole (200 mg) was added to the solution, and the reaction mixture was heated at 50 °C overnight. The mixture was casted onto a clean and smooth glass plate at 60 °C for 24 h to produce the Br[−] form AEM. The as-prepared membrane was immersed into a 1 M NaOH aqueous solution at 25 °C for 48 h to process the hydroxide exchange completely to yield the desired OH[−] form membrane named as DIM-PPYPAES-*X* with the thickness of 40–80 μm. Herein, DIM refers to the 1,2-dimethylimidazolium functionalized membranes and *X* represents the number of 1/2/3/4 respectively with the increase of ion exchange capacity (IEC) of the membranes. The obtained OH[−] form membrane was washed with deionized water for several times and kept in deionized water before use. The total synthetic route for DIM-PPYPAES ionomers is illustrated in Scheme 2. The detailed synthetic route and characterization spectra of the DIM-PSF membrane are shown in ESI.†

2.3 Characterization of the DIM-PPYPAES membranes

2.3.1 ¹H NMR and FT-IR spectroscopy. ¹H NMR spectra were recorded on a 400 MHz spectrometer (Bruker) using tetramethylsilane as the internal standard. Deuterated dimethyl sulfoxide (DMSO-*d*₆) or deuterated chloroform (CDCl₃) was used as the solvent. FT-IR spectra of the samples were analyzed in the range of 4000–400 cm^{−1} by using a Thermo-Nicolet 6700 spectrometer.

2.3.2 Thermal stability. Thermogravimetric analyzer (Mettler Toledo TGA/DSC1) was used to evaluate the thermal stability in the temperature range 50–600 °C at a heating rate of 20 °C min^{−1} under a N₂ atmosphere. Differential scanning calorimetry (DSC) was performed to determine the glass transition temperature (*T*_g) of the samples using a DSC Q2000 analyzer from TA Instruments. DSC heating/cooling/heating temperature was from 50 °C to 280 °C, however, the data recorded and *T*_g was determined from the second heating cycle to eliminate the thermodynamic history.

2.3.3 Mechanical property. The mechanical properties of the PPYPAES resin, the DIM-PPYPAES-1/2/3/4 membranes and the DIM-PSF membrane were studied using a universal testing machine (Instron 5567 testing system) with a crosshead speed of 10 mm min^{−1} at room temperature and 40% RH. A 10 mm wide membrane was kept in deionized water at 25 °C overnight and was taken out to remove the surface water using a tissue before the measurements.

2.3.4 Water uptake and swelling ratio. The water uptake of the membrane was measured by immersing the membrane sample in deionized water at 30 °C (or 60 °C) for 24 h. Then, the membrane was taken out, and the excess water on the surface was wiped out by using absorbent paper and weighed immediately. Afterwards, the membrane was dried *in vacuo* at 60 °C for at least 48 h, and the membrane was weighed again until the weight was invariable. The water uptake was calculated according to the following equation:

$$\text{WU}(\%) = \frac{M_{\text{wet}} - M_{\text{dry}}}{M_{\text{dry}}} \times 100\%$$

where *M*_{wet} and *M*_{dry} are the mass of the membrane in the wet and dry states, respectively.

The dimensional change of the membranes was evaluated by measuring the swelling ratio, and the changes of both through-plane and in-plane directions were calculated by using the following equations:

$$\text{SR}_{\text{i-p}}(\%) = \frac{L_{\text{wet}} \times W_{\text{wet}} - L_{\text{dry}} \times W_{\text{dry}}}{L_{\text{dry}} \times W_{\text{dry}}} \times 100\%$$

$$\text{SR}_{\text{t-p}}(\%) = \frac{T_{\text{wet}} - T_{\text{dry}}}{T_{\text{dry}}} \times 100\%$$

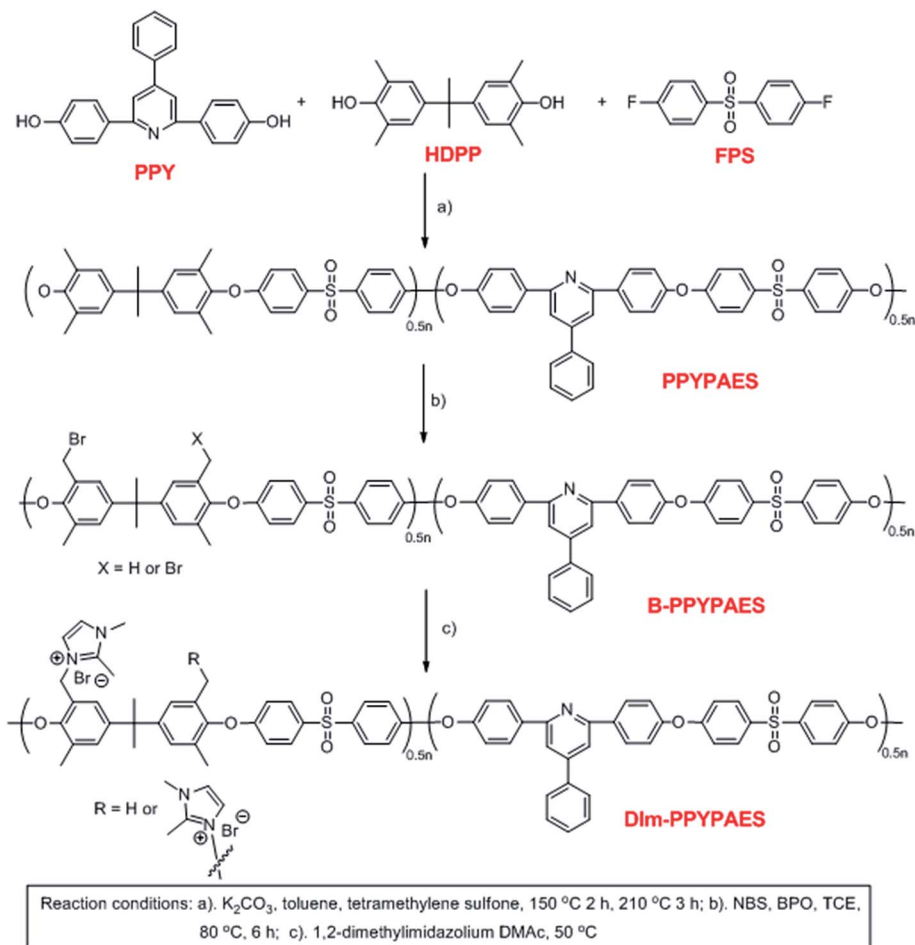
where SR_{t-p} and SR_{i-p} refer to changes of through-plane and in-plane directions, respectively; *L*_{wet}, *W*_{wet} and *T*_{wet} are the length, width and thickness of the wet membranes, respectively, and *L*_{dry}, *W*_{dry} and *T*_{dry} are the length, width and thickness of the dried membranes, respectively.

2.3.5 Ion exchange capacity (IEC). To obtain the measured IEC value, the Br[−] form AEM was immersed in 25 mL of a 1 M NaNO₃ solution for 48 h at 25 °C to undergo the complete ionic exchange process. Afterwards, the solution was titrated with a 0.1 M AgNO₃ standard solution and K₂CrO₄ (5 wt%) was used as a colorimetric indicator. The IEC (meq. g^{−1}) was calculated using the following equation:

$$\text{IEC}(\text{meq. g}^{-1}) = \frac{V_{\text{AgNO}_3} \times C_{\text{AgNO}_3}}{M_{\text{dry}}}$$

where *V*_{AgNO₃} is the volume of the consumed AgNO₃ solution, *C*_{AgNO₃} is the concentration of the AgNO₃ solution, and *M*_{dry} is the weight of the dry membrane, respectively.

2.3.6 Hydroxide conductivity. The ionic conductivities of the OH[−] form membrane samples were determined *via* AC impedance spectroscopy with Zehner electrochemical equipment (Germany) in a frequency ranging from 0.1 Hz to 100 kHz. The area resistance (*R*) of anion exchange membrane was



Scheme 2 Synthesis of PPYPAES, B-PPYPAES and DIm-PPYPAES samples.

measured at a Zehner electrochemistry working station by the two-probe method in deionized water. The ionic conductivity σ ($S\ cm^{-1}$) of the membrane sample was calculated using the following equation:

$$\sigma(S\ cm^{-1}) = \frac{L}{R \times A}$$

where L is the distance between the two electrodes (cm), R is the resistance of membrane (Ω), A is the area of the cross-section (cm^2).

2.3.7 Alkaline stability. The alkaline stability of the membranes was evaluated by soaking the membranes in a 2 M NaOH solution at 60 °C for 5, 10 and 15 days. The degradation degree of the AEMs was studied by measuring the changes of hydroxide conductivity and the IEC value. For measuring the IEC value, after 5, 10, 15 days of immersion under alkaline aqueous conditions at 60 °C, some pieces of the membranes were washed with deionized water and immersed into a 1 M NaBr solution at 25 °C for 48 h to process the Br^- exchange completely. Subsequently removing the excess salt *via* being immersed, the Br^- form membranes in deionized water for 48 h before measurement of the IEC value.

3. Results and discussion

3.1 Synthesis and characterization of the PPYPAES resin and the DIm-PPYPAES membranes

The synthetic route for the DIm-PPYPAES membranes is shown in Scheme 2. We utilized the equivalent mole ratio of 2,2-bis(4-hydroxy-3,5-dimethylphenyl)propane (HDPP) and 4-phenyl-2,6-bis(4-hydroxyphenyl)pyridine (PPY) monomers to yield a random copolymer containing the 4-phenyl-pyridine moiety in the main chain. After radical bromination and subsequent functionalization with 1,2-dimethylimidazolium, a series of flexible, ductile and transparent membranes could be obtained by casting the solution of DIm-PPYPAES in the DMAc onto a smooth and clean glass plate at 60 °C. Immersing the Br^- form membranes into a 1 M NaOH aqueous solution for 48 h to yield the desired OH^- form DIm-PPYPAES membranes.

3.2 1H NMR and FT-IR spectroscopy

Fig. 1a shows the 1H NMR spectrum of the synthesized resin. All the protons on the polymer backbone and their corresponding signals in the spectrum were identified in detail. The strong single peak at 2.0 ppm was the typical signal of the benzyl moiety without any substituents. The clear signal at 8.2

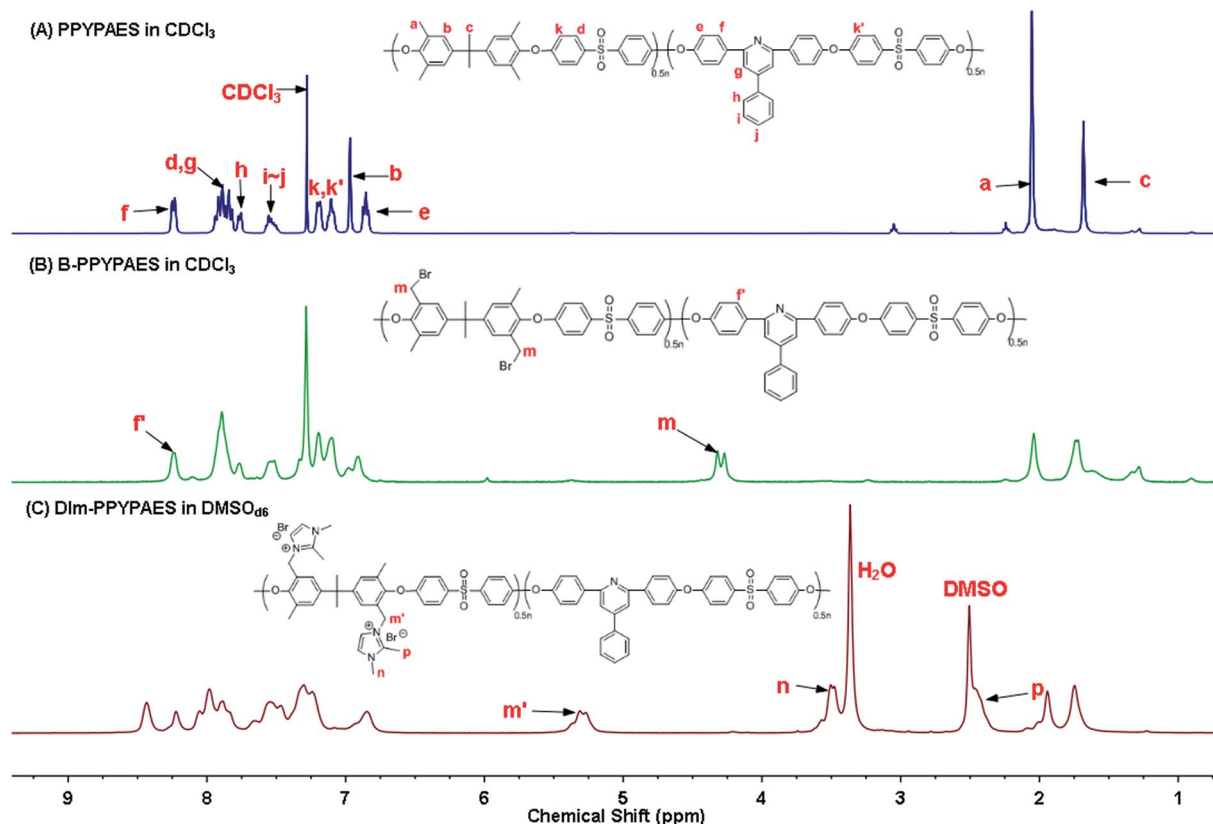


Fig. 1 ^1H NMR spectra of (a) PPYPAES in CDCl_3 , (b) B-PPYPAES in CDCl_3 and (c) DIm-PPYPAES in $\text{DMSO}-d_6$.

ppm was ascribed to the protons of phenyl that attached to the *ortho* position of the pyridine ring, indicating the successful construction of the expected polymer backbone. In addition, the multi-peaks at around 7.9 ppm were partially attributed to the protons of the phenyl ring at the *ortho* position of the sulfone group, and the others were the signal of the protons at the *meta* position of pyridine. After the radical bromination reaction, it can be seen from Fig. 1b that the typical peak of the bromo-benzyl group appeared at 4.2 ppm, indicating that the bromination reaction was processed successfully. In Fig. 1c, the broad peak at 5.2 ppm responded to the changes of methylene after the substitution of bromo atom by the 1,2-dimethylimidazolium group. Meanwhile, both peaks appeared at 3.5 ppm and 2.4 ppm, which could also indirectly demonstrate the successful introduction of the pendant ionic group. Moreover, Fourier transform infrared (FT-IR) spectroscopy was also employed to further identify the structure of the prepared membranes (Fig. S2†). The peaks at 1580 cm^{-1} were attributed to the vibrational mode of the imidazolium ring. Absorption peaks at 1240 cm^{-1} confirmed the existence of aryl ethers. Compared with the spectra of the PPYPAES and the B-PPYPAES samples, a broad and strong peak at around 3382 cm^{-1} was ascribed to the stretching vibration of the hydroxyl group, indicating the successful exchange of the Br^- ion to the OH^- ion. The chemical structure of the DIm-PSF membrane was confirmed by the ^1H NMR spectrum as shown in Fig. S4.†

3.3 Thermal stability

The thermal stability of the PPYPAES copolymer and the DIm-PPYPAES membranes in the Br^- form was evaluated by using thermogravimetric analysis (TGA). The TGA curves were recorded from 50°C to 800°C under N_2 flow at a heating rate of $20^\circ\text{C min}^{-1}$. As shown in Fig. 2, for the PPYPAES copolymer, one sharp weight loss process occurred at around 420°C ; this value

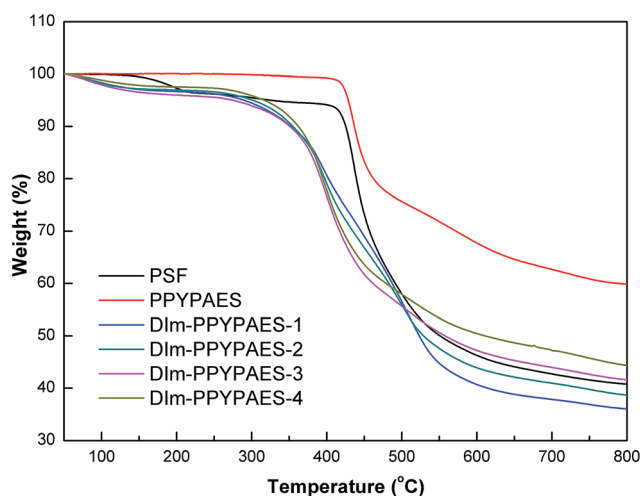


Fig. 2 TGA curves of the PSF and the PPYPAES polymer and the DIm-PPYPAES-1/2/3/4 membranes.

represents the degradation temperature of the PPYPAES backbone. Moreover, every DIM-PPYPAES membrane demonstrated a typical and obvious three stages of weight loss, respectively. The first weight loss was less than 5% below 150 °C, probably due to the evaporation of the water molecules in the membrane. The second stage of weight loss was initiated from 280 °C, and the decomposition of the pendant 1,2-dimethylimidazolium groups could explain this weight loss stage. The degradation of the polymer backbone that occurred above 410 °C was the only reason for the third stage of dramatic weight loss. These results firmly indicated that the as-prepared DIM-PPYPAES membranes possess sufficient thermal stability for practical application in fuel cells.

Fig. 3 shows the glass transition temperature T_g of the PPYPAES resins and the PPYPAES derived membranes. For every sample, only one T_g was observed in the whole temperature range. The T_g of the PPYPAES polymer was 230.6 °C, with the increase of ionic groups on per repeating unit (IEC), the T_g of the membranes (in Br⁻ form) exhibited a slight increasing trend from 235.4 °C to 243.2 °C. This finding indicated that with the increased introduction of rigid 1,2-dimethylimidazolium groups into the polymer, a stronger interaction between pendant ionic groups was benefited, which might further hinder the movement of polymer chains and elevate the T_g .

In addition, for a comprehensive evaluation of the effect of the introduction of the PPY unit into the polymeric backbone, the thermal behavior of the PSF copolymer without the PPY unit was investigated as well. It can be seen from Fig. 2 and 3 that the degradation temperature and glass transition temperature of the PSF polymer was 410 °C and 226.5 °C, respectively, which were slightly lower than those of the PPYPAES resin. This result implied that the incorporation of the 4-phenyl-pyridine moiety enhanced the thermal stability.

3.4 Mechanical property and solubility behavior

The mechanical properties and corresponding experimental errors of the PPYPAES, DIM-PPYPAES and DIM-PSF membranes

are summarized in Table 1. These samples exhibited values of tensile stress in the range of 21.1–46.2 MPa, and elongation at the break ranging from 5.4% to 15.2% at 40% RH. Furthermore, the tensile stress of the membranes was enhanced with increasing IEC value. The mechanical results of the produced membranes were tough enough for potential use as AEM materials.

Table 2 shows the solubility behavior of the PPYPAES, DIM-PPYPAES and DIM-PSF samples in various organic solvents and deionized water. It can be seen that the PPYPAES resin was well soluble in most of aprotic solvents, such as DMF, CH₂Cl₂, CHCl₃, THF and DMAc, *etc.* while both AEMs were soluble in aprotic polar solvents. The good solubility of PPYPAES in these organic solvents might facilitate the wider application of the synthesized polymers.

3.5 Morphology of the membranes

The morphology of the OH⁻ form DIM-PPYPAES membranes was examined by employing atomic force microscopy (AFM) and scanning electron microscopy (SEM). Fig. 4 shows the AFM phase images of the DIM-PPYPAES-1 and DIM-PPYPAES-4 membranes. The clear hydrophobic-hydrophilic domain separation could be observed in the two phase images probably due to the incorporation of the 4-phenyl-pyridine moieties as the hydrophobic rigid side chains, enhancing the self-aggregated influence on the different ionic clusters. Meanwhile, compared with the DIM-PPYPAES-1 membrane with an IEC of 1.15 meq. g⁻¹, the DIM-PPYPAES-4 membrane with a higher IEC of 1.77 meq. g⁻¹ exhibited larger hydrophilic domains (dark region), mainly composed of water molecules and 1,2-dimethylimidazolium clusters, facilitating the formation of interconnected nanostructured channels. Combining the DSC results as shown in Fig. 3, we can see that with the introduction of the PPY unit and an increase of pendant 1,2-dimethylimidazolium salts, the interaction between different polymeric chains was strengthened. This would greatly facilitate the aggregation of ionic clusters and formation of efficient ionic channels, which was beneficial to the ionic conductivity. Furthermore, the morphology of the surface and cross-section of the membrane examined by the SEM technique are shown in Fig. S6.† A uniform, compact and smooth surface and a thickness value of approximately 40 μm of the membrane could be clearly observed.

3.6 Ionic conductivity, water uptake and dimensional stability

High hydroxide conductivity is always a key and required property for the alkaline anion exchange membranes. The conductivities of the DIM-PPYPAES membranes in OH⁻ form were measured under fully hydrated conditions, and the curves are shown in Fig. 5. We can see that the hydroxide conductivities increased gradually with increasing temperature. In general, the membrane with relatively high IEC is beneficial for obtaining good hydroxide conductivity. For example, the DIM-PPYPAES-4 membrane with an IEC value of 1.77 meq. g⁻¹, showed a higher level of ionic conductivity than those of the

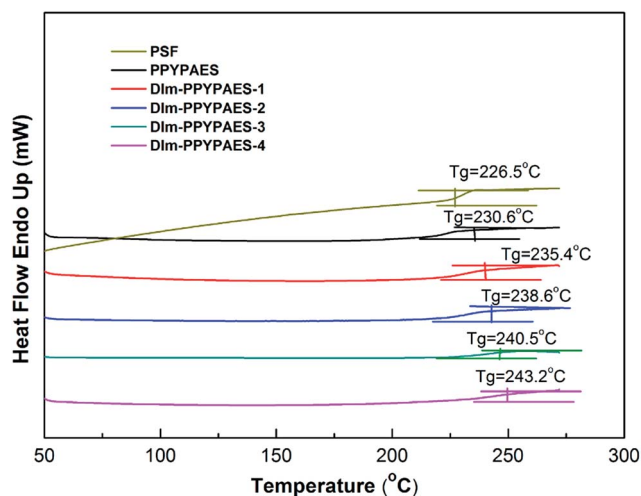


Fig. 3 DSC curves of the PSF and the PPYPAES copolymers and the DIM-PPYPAES-1/2/3/4 membranes.

Table 1 Mechanical properties^a

Sample	Tensile strength (MPa)	Young's modulus (MPa)	Elongation at break (%)
PPYPAES	41.2 ± 6.7	1280.8 ± 63.6	7.3 ± 0.9
DIm-PPYPAES-1	21.1 ± 1.4	660.5 ± 30.3	6.8 ± 1.7
DIm-PPYPAES-2	29.2 ± 1.8	1097.8 ± 73.5	7.1 ± 0.8
DIm-PPYPAES-3	37.5 ± 4.7	1484.2 ± 128.2	5.4 ± 1.1
DIm-PPYPAES-4	46.2 ± 2.3	1938.3 ± 67.3	6.6 ± 1.9
DIm-PSF	49.1 ± 6.9	986.5 ± 32.4	15.2 ± 3.4

^a Measured at 25 °C and 40% RH, averaged from two trials.

other three membranes with lower IEC values, achieving 33.33 mS cm⁻¹ at 30 °C and 83.35 mS cm⁻¹ at 80 °C. Furthermore, both water uptake and dimensional stability are also important parameters to evaluate the AEM materials. From Fig. 6 and 7, it can be found that all the water uptake and swelling behaviors in-plane directions SR_{i-p} for the DIm-PPYPAES membranes in Br⁻ form remained below 20% and 10% at 30 °C and 60 °C, respectively. After the anion exchanging of Br⁻ to OH⁻, much higher water uptakes and swelling ratios for the DIm-PPYPAES membranes were obtained, which were mainly due to the stronger hydrophilicity of the OH⁻ ion. Temperature dependence of ionic conductivity of the DIm-PSF membrane was also investigated and shown in Fig. S7.† Unfortunately, when the temperature was heated above 70 °C, the membrane decomposed into several small pieces owing to a swelling degree that was too high.

Herein, for the purpose of further illustrating the influence on the properties from the incorporation of the bulky 4-phenyl-pyridine unit in the main chain, comparisons of hydroxide conductivity, water uptake and dimensional stability between the DIm-PPYPAES membranes, DIm-PSF membranes and other previously reported imidazolium containing membranes are listed in Table 3. It can be seen that, although the DIm-PSF membrane had a higher IEC of 2.26 meq. cm⁻¹ as well as other reported AEMs with a similar IEC level, they still exhibited lower ionic conductivity than that of the DIm-PPYPAES-4 membrane at 30 °C. Moreover, the DIm-PSF membrane decomposed into several pieces when the temperature of the ionic conductivity measured was above 70 °C. It might be explained by the “self-aggregation” model where the introduction of the bulky hydrophobic 4-phenyl-pyridine moiety as a rigid side chain between different polymer chains further benefits the formation of large ionic clusters, which significantly enhanced the ion transport efficiency. As a result,

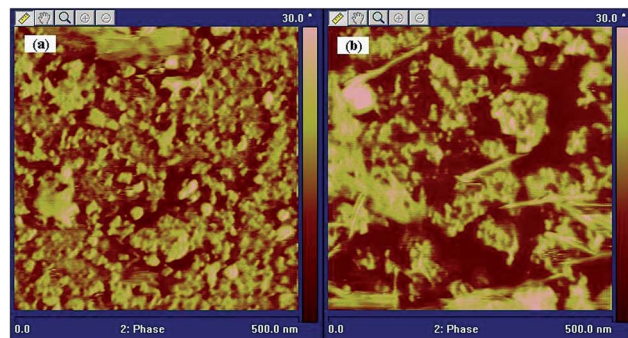


Fig. 4 AFM phase images of (a) DIm-PPYPAES-1 (IEC: 1.15 meq. g⁻¹) and (b) DIm-PPYPAES-4 (IEC: 1.77 meq. g⁻¹) membranes in the OH⁻ form.

compared with the listed benzylmethylimidazolium (BMI)-head type membranes with similar or higher IEC values as benchmarks, the DIm-PPYPAES membranes containing a PPY unit in the backbone possessed superior hydroxide conductivities.

3.7 Long-term alkaline stability

The alkaline stability is another critical property for evaluating the performance of AEMs. We investigated the long-term alkaline stability of the produced membranes by immersing the membranes into a N₂ saturated 2 M NaOH aqueous solution at 60 °C for several days, and examining the changes of ionic conductivities and IEC values before and after the treatment with a strong alkaline aqueous solution (shown in Fig. 8 and S7†). It could be obviously seen that both the hydroxide conductivity and IEC value decreased dramatically after immersion under strong alkaline conditions for 5 days. After 10 and 15 days, a trend of slight decreasing and/or invariable for

Table 2 Solubility behavior^a

Samples	CH ₂ Cl ₂	CHCl ₃	NMP	DMF	DMSO	DMAc	THF	EtOH	H ₂ O
PPYPAES	++ ^b	++	++	++	+— ^d	++	++	—	—
DIm-PPYPAES-4	— ^c	—	++	++	++	++	—	—	—
DIm-PSF	—	—	++	++	++	++	—	—	—

^a The solubility behavior was studied by immersing the sample into the solvent with the concentration of 5 mg/1 mL for 24 h. ^b ++ represents completely soluble at 25 °C. ^c — represents insoluble even at 60 °C. ^d +— represents partially soluble at 60 °C.

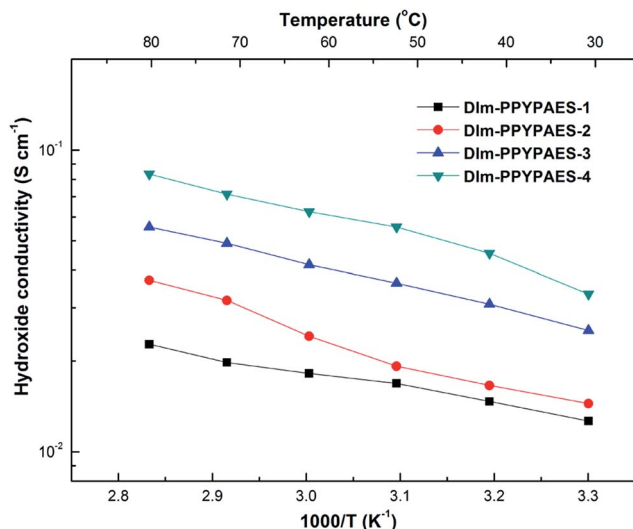


Fig. 5 Hydroxide conductivity of the produced DIm-PPYPAES membranes as a function of temperature under fully hydrated conditions.

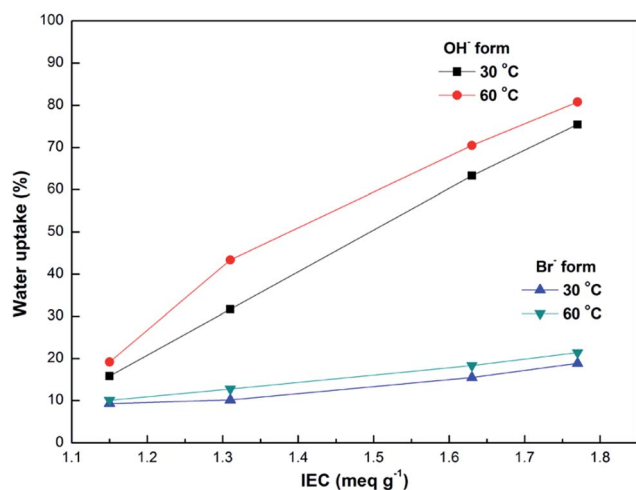


Fig. 6 IEC dependence of water uptake of the DIm-PPYPAES membranes in both Br⁻ and OH⁻ forms after immersion in deionized water at certain temperatures.

the DIm-PPYPAES-4 membrane was observed, while the ionic conductivity of the DIm-PSF still decreased dramatically. This was probably due to the degradation of pendant 1,2-dimethylimidazolium groups which were attacked by surrounding OH⁻ ions. This finding is very different from some results which reported that the membranes or small organic molecules containing C2-alkyl substituted imidazoliums possess excellent alkaline stability attributed to the steric hindrance effect of the C2-position substituent.^{42,43} Considering the imidazolium functionalized membranes with various polymer backbones and different grafting mode (spacer or no-spacer) of pendant imidazolium groups onto the main chain, there might be structure-selectivity relationships between the pendant ionic groups and the polymeric main chains. This indicates that

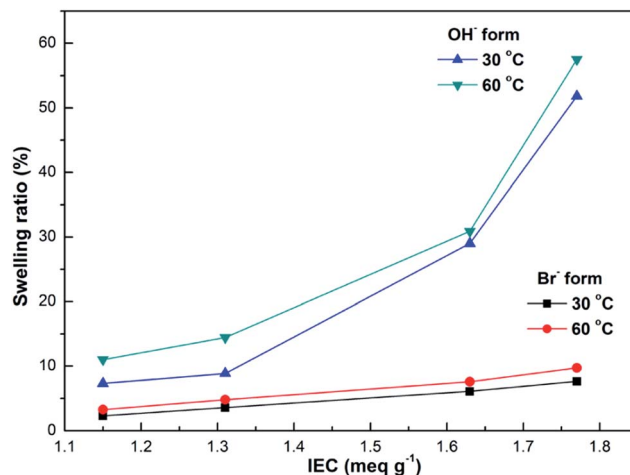


Fig. 7 IEC dependence of SR_{i-p} of the DIm-PPYPAES membranes in both Br⁻ and OH⁻ forms after immersing in deionized water at a given temperature.

a comprehensive screening on the aforementioned factors is necessary to obtain an optimized structure of the membrane with excellent alkaline stability. Consequently, it promotes us to further explore and screen more kinds of ionic groups to fulfill the requirement of this pyridine unit based membranes with high alkaline stability.

In addition, we also found that, among all the measured anion exchange membranes, the DIm-PPYPAES-4 membrane with an IEC value of 1.77 meq. g⁻¹ still exhibited good ionic conductivity above 10 mS cm⁻¹ at 30 °C which was higher than that of the DIm-PSF membrane after the treatment with alkaline conditions at elevated temperature for 15 days. Moreover, it should be noted that although the ionic conductivity and IEC value decreased significantly, none of membranes decomposed to small pieces. In particular, the DIm-PPYPAES-4 membrane still retained its compact and flexible property as well as integrated shape (shown in Fig. S8†). These findings indicated that the DIm-PPYPAES membranes were of good stability under the elevated temperature and fully hydrated environment, and showed reasonable alkaline durability. Compared with the conventional cardo-based poly(arylene ether sulfone)s, incorporation of the pyridine scaffold to replace the quaternary carbon center could partially alleviate the cation induced degradation of the polymer backbone affected by hydrolysis, because the sp³ hybrid carbon center is prone to be attacked compare to the aromatic rings under alkaline conditions, usually resulting in the decomposition of the membranes into small pieces.⁴⁴

4. Conclusion

In summary, we designed and synthesized a new series of 4-phenyl-pyridine unit containing poly(arylene ether sulfone)s functionalized with 1,2-dimethylimidazolium for use as alkaline anion exchange membranes. It was found that the incorporation of the 4-phenyl-pyridine moiety into the polymeric

Table 3 IEC, water uptake, swelling ratio and conductivity σ of the membranes

Sample	IEC (meq. g ⁻¹)		WU (%) ^c		SR _{t-p} ^{c,d} (%)		σ (mS cm ⁻¹) 30 °C
	Cal. ^a	Exp. ^b	30 °C	60 °C	30 °C	60 °C	
DIm-PPYPAES-1	1.22	1.15	17.94	22.17	7.89 (6.98)	12.12 (9.67)	12.63
DIm-PPYPAES-2	1.33	1.31	30.42	46.76	8.87 (7.11)	19.32 (17.42)	14.43
DIm-PPYPAES-3	1.64	1.63	67.65	78.22	30.13 (26.12)	36.79 (31.21)	25.25
DIm-PPYPAES-4	1.82	1.77	78.53	87.24	55.43 (49.34)	59.31 (53.76)	33.33
DIm-PSF	2.86	2.26	102.35	126.54	75.72	86.89	30.60
PSF-ImmOH-60 ^e	—	1.79	47	88	26	41	11
PES-MeIm/OH-#5 ^f	—	1.65	120	—	46.2	—	9.6
DIm-PPO-0.30 ^g	—	1.96	65.9	—	17.8	—	20

^a Calculated from ¹H NMR spectra. ^b Measured by the titration method. ^c The as-prepared OH⁻ form membranes were measured at a given temperature from two trials. ^d SR_{t-p} values are in parentheses. ^e Ref. 15. ^f Ref. 40. ^g Ref. 41.

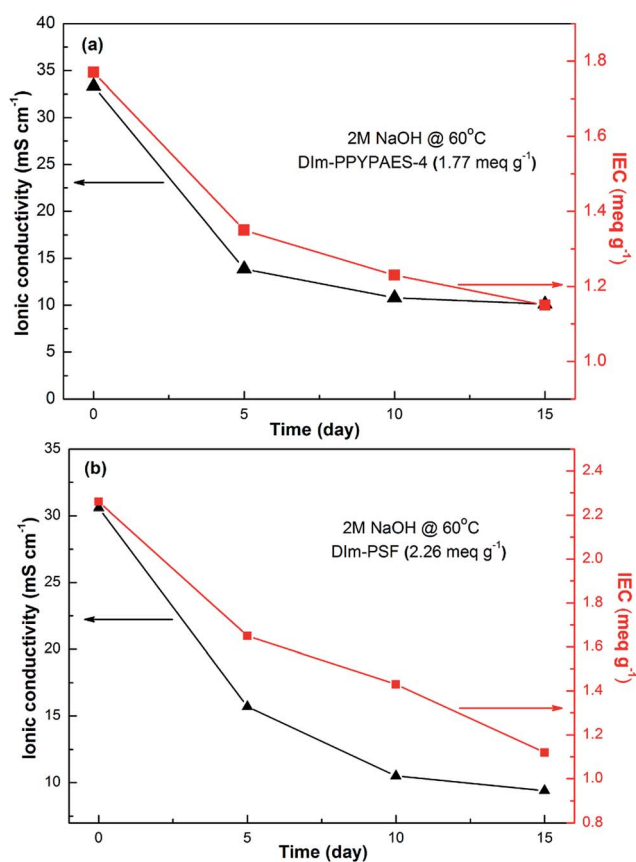


Fig. 8 The changes of ionic conductivity and IEC of the (a) DIm-PPYPAES-4, (b) DIm-PSF membranes before and after immersion in a 2 M NaOH solution at 60 °C.

backbone would facilitate the formation of large ionic clusters, and the fabricated DIm-PPYPAES membranes consequently exhibited enhanced ionic conductivity compared to the DIm-PSF membrane. A relatively high level of hydroxide conductivities was observed for the DIm-PPYPAES membranes with different IECs of 1.15–1.77 meq. g⁻¹. Among all the samples, the DIm-PPYPAES-4 membrane achieved the highest hydroxide conductivity of 83.35 mS cm⁻¹ at 80 °C with an experimental IEC of 1.77 meq. g⁻¹. The DIm-PPYPAES membranes also

showed good solubility behavior in most of the organic solvents and high thermal stability. After being immersed in a 2 M NaOH aqueous solution at 60 °C for 15 days, the hydroxide conductivities of the DIm-PPYPAES membranes decreased in varying degrees, but the DIm-PPYPAES-4 membrane still exhibited conductivity above 10 mS cm⁻¹ at 30 °C, while all the DIm-PPYPAES membranes retained their flexible property and original integrated shapes. This result provided us a clue that the produced copolymer containing a pyridine moiety (PPYPAES) possesses great potential application in fuel cells or other separation and purification technologies.

Acknowledgements

The authors greatly appreciate the financial support by Zhejiang Provincial Natural Science Foundation of China (No. LY15B020003), Ningbo Natural Science Foundation (No. 2015A610243), the “Membranes for Environmental Remediation” Innovation Team from Ningbo Technology Bureau (No. 2014B81004) and the “Membrane and Water Treatment” 2011 Coherence Innovation Center of Zhejiang Province.

References

- 1 B. C. Steele and A. Heinzl, *Nature*, 2001, **414**, 345.
- 2 M. Z. Jacobson, W. G. Colella and D. M. Golden, *Science*, 2005, **308**, 1901.
- 3 J. R. Varcoe and R. C. T. Slade, *Fuel Cells*, 2005, **5**, 187.
- 4 H. Zhang, D. Chen, Y. Xianze and S. Yin, *Fuel Cells*, 2015, **15**, 761.
- 5 S. Lu, J. Pan, A. Huang, L. Zhuang and J. Lu, *Proc. Natl. Acad. Sci. U. S. A.*, 2008, **105**, 20611.
- 6 C. Yang, S. Wang, W. Ma, L. Jiang and G. Sun, *J. Mater. Chem. A*, 2015, **3**, 8559.
- 7 B. Lin, H. Dong, Y. Li, Z. Si, F. Gu and F. Yan, *Chem. Mater.*, 2013, **25**, 1858.
- 8 H. S. Dang and P. Jannasch, *Macromolecules*, 2015, **48**, 5742.
- 9 J. Ran, L. Wu, Q. Ge, Y. Chen and T. Xu, *J. Membr. Sci.*, 2014, **470**, 229.
- 10 Q. Li, L. Liu, Q. Miao, B. Jin and R. Bai, *Chem. Commun.*, 2014, **50**, 2791.

- 11 N. Li, Y. Leng, M. A. Hickner and C. Wang, *J. Am. Chem. Soc.*, 2013, **135**, 10124.
- 12 Z. Yang, J. Zhou, S. Wang, J. Hou, L. Wu and T. Xu, *J. Mater. Chem. A*, 2015, **3**, 15015.
- 13 M. R. Hibbs, C. H. Fujimoto and C. J. Cornelius, *Macromolecules*, 2009, **42**, 8316.
- 14 L. Jheng, S. L. Hsu, B. Lin and Y. Hsu, *J. Membr. Sci.*, 2014, **460**, 160.
- 15 Y. Yang, J. Wang, J. Zheng, S. Li and S. Zhang, *J. Membr. Sci.*, 2014, **467**, 48.
- 16 J. Yan and M. A. Hickner, *Macromolecules*, 2010, **43**, 2349.
- 17 S. Gu, R. Cai, T. Luo, Z. Chen, M. Sun, Y. Liu, G. He and Y. Yan, *Angew. Chem., Int. Ed.*, 2009, **48**, 6499.
- 18 J. Pan, S. Lu, Y. Li, A. Huang, L. Zhuang and J. Lu, *Adv. Funct. Mater.*, 2010, **20**, 312.
- 19 F. Zhang, H. Zhang and C. Qu, *J. Mater. Chem.*, 2011, **21**, 12744.
- 20 X. Yan, S. Gu, G. He, X. Wu and J. Benziger, *J. Power Sources*, 2014, **250**, 90.
- 21 J. Pan, C. Chen, L. Zhuang and J. Lu, *Acc. Chem. Res.*, 2012, **45**, 473.
- 22 J. Pan, Y. Li, L. Zhuang and J. Lu, *Chem. Commun.*, 2010, **46**, 8597.
- 23 S. Gu, R. Cai and Y. Yan, *Chem. Commun.*, 2011, **47**, 2856.
- 24 A. N. Rao, S. Nam and T. Kim, *J. Mater. Chem. A*, 2015, **3**, 8571.
- 25 X. Li, G. Nie, J. Tao, W. Wu, L. Wang and S. Liao, *ACS Appl. Mater. Interfaces*, 2014, **6**, 7585.
- 26 K. Miyatake, B. Bae and M. Watanabe, *Polym. Chem.*, 2011, **2**, 1919.
- 27 M. Tanaka, M. Koike, K. Miyatake and M. Watanabe, *Macromolecules*, 2010, **43**, 2657.
- 28 M. Tanaka, K. Fukasawa, E. Nishino, S. Yamaguchi, K. Yamada, H. Tanaka, B. Bae, K. Miyatake and M. Watanabe, *J. Am. Chem. Soc.*, 2011, **133**, 10646.
- 29 W. H. Lee, A. D. Mohanty and C. Bae, *ACS Macro Lett.*, 2015, **4**, 453.
- 30 D. Chen and M. A. Hickner, *ACS Appl. Mater. Interfaces*, 2012, **4**, 5775.
- 31 A. Lai, L. Wang, C. Lin, Y. Zhuo, Q. Zhang, A. Zhu and Q. Liu, *ACS Appl. Mater. Interfaces*, 2015, **7**, 8284.
- 32 Q. Zhang, S. Li and S. Zhang, *Chem. Commun.*, 2010, **46**, 7495.
- 33 X. Li, Y. Yu, Q. Liu and Y. Meng, *ACS Appl. Mater. Interfaces*, 2012, **4**, 3627.
- 34 X. Li, Y. Yu, Q. Liu and Y. Meng, *J. Membr. Sci.*, 2013, **436**, 202.
- 35 S. Zhang, B. Zhang, D. Xing and X. Jian, *J. Mater. Chem. A*, 2013, **1**, 12246.
- 36 S. Zhang, B. Zhang, G. Zhao and X. Jian, *J. Mater. Chem. A*, 2014, **2**, 3083.
- 37 J. Liu, L. Wang, H. Yang, Y. Li and S. Yang, *J. Polym. Sci., Part A: Polym. Chem.*, 2004, **42**, 1845.
- 38 S. Banerjee, M. K. Madhra, A. K. Salunke and D. K. Jaiswal, *Polymer*, 2003, **44**, 613.
- 39 Y. Shang, L. Fan, S. Yang and X. Xie, *Eur. Polym. J.*, 2006, **42**, 981.
- 40 W. Lu, Z. Shao, G. Zhang, Y. Zhao, J. Li and B. Yi, *Int. J. Hydrogen Energy*, 2013, **38**, 9285.
- 41 X. Lin, J. R. Varcoe, S. D. Poynton, X. Liang, A. L. Ong, J. Ran, Y. Li and T. Xu, *J. Mater. Chem. A*, 2013, **1**, 7262.
- 42 B. Lin, L. Qiu, B. Qiu, Y. Peng and F. Yan, *Macromolecules*, 2011, **44**, 9642.
- 43 S. C. Price, K. S. Williams and F. L. Beyer, *ACS Macro Lett.*, 2014, **3**, 160.
- 44 C. G. Arges and V. Ramani, *Proc. Natl. Acad. Sci. U. S. A.*, 2013, **110**, 2490.